Available online at www.sciencedirect.com
SCIENCE DIRECT®
Catalysis Today 93–95 (2004) 27–38
CATALYSIS TODAY
www.elsevier.com/locate/cattod

Carbon nanotubes-supported Ru catalyst for the generation of CO_x-free hydrogen from ammonia

S.F. Yin [a,b,d], B.Q. Xu [b,*], W.X. Zhu [a,c], C.F. Ng [a], X.P. Zhou [d], C.T. Au [a,*]

[a] *Department of Chemistry, Centre for Surface Analysis and Research, Hong Kong Baptist University, Kowloon Tong, Hong Kong, China*
[b] *Innovative Catalysis Program, Key Laboratory of Organic Optoelectronics & Molecular Engineering, Department of Chemistry, Tsinghua University, Beijing 100084, China*
[c] *Department of Chemistry, Xiamen University, Xiamen 361005, China*
[d] *Department of Chemical Engineering, Hunan University, Changsha 410006, China*

Available online 3 July 2004

Abstract

In comparison to Ru catalysts supported on activated carbon (AC), MgO, Al_2O_3, and TiO_2 under similar reaction conditions, Ru catalyst using carbon nanotubes as support (Ru/CNTs) was found to show high NH_3 conversion for the generation of CO_x-free hydrogen from NH_3. The modification of the catalyst with KOH leads to a significant improvement in activity, either in term of NH_3 conversion or TOF. The Ru/CNTs catalyst prepared from acetone solvent is more active than that from water solvent, and the use of the former leads to an increase in Ru dispersion and a decrease in residual Cl concentration. The results of H_2-TPD and HRTEM characterization disclosed that the excellent catalytic activity of Ru/CNTs could be ascribed to the high dispersion of Ru particles, and to the high graphitization and high purity of the CNTs material. The residual Cl originated from the $RuCl_3$ precursor was found to be a strong inhibitor for the decomposition reaction. Once the residual Cl is in the form of KCl, it is difficult to remove. The results of N_2-TPD studies imply that the desorption of N_2 is the rate-determining step, and the modification with KOH leads to a decrease in N_2 desorption temperature and in apparent activation energy of NH_3 decomposition over Ru/CNTs.

Keywords: Ruthenium catalyst; Carbon nanotubes; Ammonia decomposition; Hydrogen manufacture

1. Introduction

For reducing pollution arising from automobile exhaust and small-scale power generation units, researches on on-site generation of hydrogen for proton exchange membrane fuel cells (PEMFC) has been conducted [1]. The hydrogen generated from carbonaceous substances (e.g. methanol, methane) inevitably accompanied with CO_x ($x = 1, 2$) that degrades the cell even at extremely low concentration [2–6]. The use of ammonia as a hydrogen provider appears to be attractive because there is no CO_x generation, and the unconverted NH_3 can be reduced to less than 200 ppb level by means of an adsorber [1]. In addition, compared to methanol reforming, NH_3 decomposition is more economical [7,8]. In the last century, most of the works conducted on NH_3 decomposition were related to NH_3 synthesis and/or NH_3 abatement [9–18]. To study the kinetics of NH_3 synthesis, researches on NH_3 decomposition were performed in diluted NH_3. Recently, there were reports on H_2 generation from pure NH_3 [19–26]. However, catalytic activities were low even at 873 K. It is necessary to develop catalysts for complete decomposition of NH_3 at lower temperatures. Based on thermodynamic constants [27], it is estimated that NH_3 equilibrium conversion at 673 K is 99.1%. Therefore, it is possible to develop an active catalyst for NH_3 decomposition at around this temperature.

In the past decades, a great amount of works has been done on NH_3 synthesis, including catalyst preparation, characterization, kinetic study and so on [28–50]. An important breakthrough was the invention of carbon-based Ru catalysts that have been commercialized in the middle of 1990s, but scientific information has not been disclosed [51]. Compared

* Corresponding authors. Tel.: +86 852 3411 7067 (C.T. Au)/+86 10 62792122 (B.Q. Xu);
fax: +86 852 3411 7348 (C.T. Au)/+86 10 62792122 (B.Q. Xu).
E-mail addresses: pctau@hkbu.edu.hk, bqxu@mail.tsinghua.edu.cn (B.Q. Xu).

0920-5861/$ – see front matter © 2004 Elsevier B.V. All rights reserved.
doi:10.1016/j.cattod.2004.05.011

to the conventional Fe-based catalysts, the Ru catalysts are more active. There are publications on factors that influence the catalytic performance of the carbon-based catalysts, e.g. support modification, Ru precursor, alkaline earth or alkali metal compound as promoter or promoter precursor, preparation method, etc. [33–36,39,44,46–50]. The accumulated knowledge on the synthesis is very important for the development of decomposition catalysts, because the synthesis and decomposition are reversible reactions. It was reported that a Ru/C catalyst of high activity and stability required a significant graphitization degree of carbon support [46,50]. Carbon nanotubes (CNTs) is a special kind of carbon materials, with structures derived from rolled graphite sheets [52]. Since its discovery, CNTs has attracted much attention in fundamental and applied researches. Of particular interest in catalysis is the potential use of CNTs as a support for metal catalysts [53–56]. Lately, papers on the use of CNTs or graphitic nanofilaments as supports for Ru catalysts in NH_3 synthesis were published, the catalysts showed activities higher than those of the Ru catalysts supported on other carbon materials [55,56]. However, there have been no publications involving the application of CNTs as a catalyst support for NH_3 decomposition.

Here, we present Ru/CNTs as a catalyst for hydrogen generation from ammonia with comparison to Ru catalysts supported on activated carbon (AC), MgO, Al_2O_3, and TiO_2. The KOH-modification of Ru/CNTs is also reported. In the course of the study, HRTEM, XPS, TPR, H_2-TPH, and H_2 (N_2)-TPD techniques were used to examine the essential factors that influence the catalysis.

2. Experimental

2.1. Catalyst preparation

The employed CNTs (i.d.: 3–10 nm, o.d.: 6–20 nm, ratio of length to diameter: 100–1000, specific surface area: 224 m^2/g) were prepared by CVD method using Fe/Al_2O_3 as catalyst [57]. The commercially available activated carbon (AC, 1220 m^2/g), analytic grade Al_2O_3 (159 m^2/g), MgO (24 m^2/g), and TiO_2 (6 m^2/g) were purchased from Beijing Chemical Plant. The CNTs and AC were pretreated (by refluxing) in 5 M aqueous HNO_3 solution for 2 h, and then calcined in H_2 flow at 973 K for 2 h to remove adsorbed impurities. The modified CNTs was prepared by impregnating the purified CNTs with aqueous KOH solution, followed by calcination at 773 K for 5 h in Ar flow (purity above 99.9%). As for the metal oxide supports, they were calcined in Ar flow at 873 K for 5 h prior to the loading of active component.

All the catalysts were prepared by wetness incipient impregnation with water or acetone as solvent, followed by drying at 328 K for 5 h and calcination in Ar flow at 823 K for 2 h. The analytic grade $RuCl_3 \cdot xH_2O$ precursor was purchased from Aldrich Chemical Company. The catalysts are designated as Ru/support-w (or -a), where w and a denote the use of water and acetone as solvent, respectively. For the catalysts modified by KOH, Ru–K/CNTs-a represents the catalyst prepared by impregnating "KOH-modified CNTs" with $RuCl_3$ dissolved in acetone, and K–Ru/CNTs-a the catalyst prepared by mixing the H_2-reduced (773 K, 2 h) Ru/CNTs-a catalyst with aqueous KOH solution, followed by drying (RT) and calcination (773 K, 2 h) in Ar flow.

It is noted that the theoretical loadings of the active components in the above-mentioned catalysts were 4.85×10^{-4} mol/g_{cat} (i.e. 5 wt.%). The results of XRF measurement conducted over sequence XRF-1700 X-ray fluorescent spectrometer (Shimadzu) showed that the actual loadings of Ru in the catalysts were in the range of 4.7–4.9 wt.% (ca. 4.8 wt.%). The K/Ru molar ratios of Ru–K/CNTs-a and K–Ru/CNTs-a were 1/1.

2.2. Catalytic tests

Catalytic testing was carried out on a continuous flow quartz reactor (catalyst: 100 mg, 60–80 mesh) under pure NH_3 [flow rate: 50 ml/min; $GHSV_{NH_3}$: 30,000 ml/(h g_{cat})]. Prior to the reaction, the catalyst was reduced in situ in a 25%-H_2/Ar flow at 773 K for 2 h, and then purged with a flow of pure Ar. The reaction temperature was in the range of 623–823 K. Product analysis was performed on an on-line gas chromatograph (Shimadzu) equipped with thermal detector and Poropak Q column, using Ar as carrier gas. We found that NH_3 conversion observed in a blank reactor or over the individual support was less than 1.0% at 823 K.

2.3. Catalyst characterization

HRTEM images were taken at 300 kV on FEI TECNAI Field Emission HRTEM. X-ray photoelectron spectra (C 1s and Cl 2p) were recorded with a SKL-12 spectrometer equipped with Mg Kα radiation. The residual pressure in the analytical chamber was maintained below 10^{-7} Torr during data acquisition.

Temperature-programmed reduction (TPR) was operated according to the following steps. Prior to each measurement, the sample (0.1 g) was heated from room temperature (RT) to 623 K with a heating rate of 10 K/min under Ar flow (40 ml/min), and kept at this temperature for 30 min for the removal of adsorbed impurities (e.g. H_2O). After the sample was cooled to RT, the gas flow was switched to 5% H_2/Ar (40 ml/min). Finally, TPR profiles were obtained with a temperature ramp of 10 K/min using a thermal conductivity detector. Before entering the detector, the gas from the TPR reactor was passed through a glass tube filled up with 4A molecular sieve and cooled to ca. 177 K to ensure complete elimination of water. Absolute H_2 consumption was obtained by calibrating the TPR peak areas against those of standard CuO samples. The reducibility of the loaded metal component was estimated based on the extent of H_2 consumption.

H_2-TPD experiments were carried out over the same equipment of TPR studies. Before each measurement, the sample (0.25 g) was heated to 773 K in a flow of 5% H_2–Ar at a rate of 10 K/min, and kept at this temperature for 0.5 h. After cooled to RT at a rate of 5 K/min, the sample was kept at RT for 0.5 h. Then, the 5% H_2–Ar flow was switched to pure Ar for a period of 0.5 h at RT. Finally, the catalyst was heated at a rate of 15 K/min, and H_2-TPD curve was recorded.

N_2-TPD experiment was carried out using the mass analyzer of a HP4890 GC–MS instrument as the detector. Before the measurement, the catalyst was heated at 623 K and reduced in 20% H_2–Ar at 773 K for 1 h, followed by a switch in gas flow to pure He for purging at 773 K for 30 min. Then the sample was exposed to N_2 and cooled slowly to RT and kept at RT for 20 min. Afterward, the gas flow was switched to pure He (40 ml/min). A stable baseline was established after a flow of He at RT for 30 min, and the catalyst was heated (10 K/min) and N_2-TPD curve recorded. The desorbed amount was calibrated against a standard pulse of N_2 via a sampling tube of 10 μl.

Temperature-programmed hydrogenation (TPH) was conducted on a MSC 200 mass spectrometer (Blazers). The gas for hydrogenation was pure H_2, and 10 K/min was the heating rate. Before the hydrogenation experiment, the sample was calcined at 673 K in a He flow for 0.5 h.

3. Results

3.1. Catalytic activity

Shown in Table 1 are the NH_3 conversion and H_2 formation rate over the Ru/support-w catalysts. At 673 K, conversion over Ru/CNTs-w is only 2.3%, and the H_2 formation rate is 0.8 mmol/(min g_{cat}); at 823 K, conversion is 40.6% and H_2 formation 13.6%. The conversion and H_2 formation rate over the other Ru/support-w catalysts are lower than those over Ru/CNTs-w within the temperature range of 673–823 K. Obviously, the use of water in catalyst preparation results in Ru catalysts of poor activity.

Without stating the reason, researchers used organic solvent (e.g. tetrahydrofuran, acetone) rather than water to dissolve Ru precursors [$RuCl_3$, $Ru(acac)_3$, $Ru_3(CO)_{12}$] in the preparation of Ru catalysts for NH_3 synthesis [33–36]. Fig. 1 and Table 2 depict the NH_3 conversion and H_2 formation rate over the Ru/support-a catalysts, respectively. Compared to that of Ru/support-w, NH_3 conversion and H_2 formation rate over Ru/support-a are much higher. At 673 K, conversion over Ru/CNTs-a is 17.1%, and H_2 formation is 5.7 mmol/(min g_{cat}). Since NH_3 decomposition is endothermic ($\Delta H = 46$ kJ/mol), a rise of reaction temperature would result in an enhancement in NH_3 conversion [19]. At 823 K, conversion over the Ru catalysts is close to the equilibrium value, and the H_2 formation rate over Ru/CNTs-a is up to 33.5 mmol/(min g_{cat}). Within the 623–823 K range, activities can be ranked as: Ru/CNTs-a > Ru/MgO-a > Ru/TiO_2-a ≅ Ru/AC-a ≅ Ru/Al_2O_3-a, a rise in temperature leads to an increase in absolute difference of NH_3 conversion. As the space velocities of NH_3 adopted in catalysts evaluation are identical, the change in H_2 formation rate as related to reaction temperature should follow a similar trend of NH_3 conversion (Table 2). In other words, the Ru/CNTs-a catalyst is highly active. We found that under similar reaction conditions, the performances of the Ru/support-w catalysts are comparable to those of Ni/SiO_2, Ir/SiO_2, and Ni/SiO_2–Al_2O_3 reported by Goodman and coworkers [19],

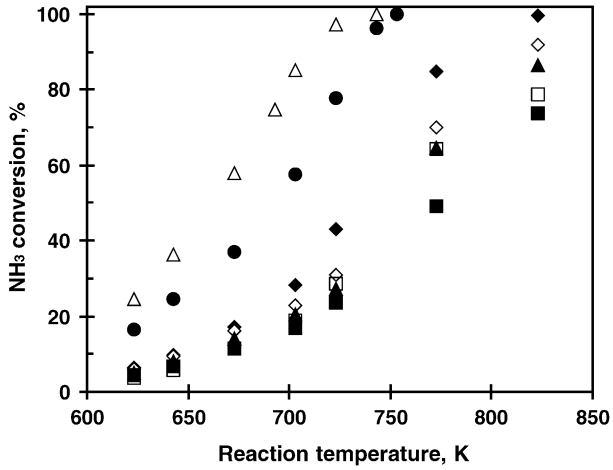

Fig. 1. NH_3 conversion as a function of reaction temperature over Ru/support-a catalysts: (◆) Ru/CNTs-a; (◇) Ru/MgO-a; (▲) Ru/TiO_2-a; (□) Ru/AC-a; (■) Ru/Al_2O_3-a; (△) K–Ru/CNTs-a; (●) Ru–K/CNTs-a. $GHSV_{NH_3}$ = 30,000 ml/(h g_{cat}), Ru loading = 4.8 wt.%.

Table 1
NH_3 decomposition over supported 4.8 wt.%-Ru catalysts using water as solvent

T, K	NH_3 conversion, %					H_2 formation rate, mmol/(min g_{cat})				
	Ru/CNTs	Ru/AC	Ru/Al_2O_3	Ru/MgO	Ru/TiO_2	Ru/CNTs	Ru/AC	Ru/Al_2O_3	Ru/MgO	Ru/TiO_2
673	2.3	0.8	2	2.4	1.9	0.8	0.3	0.6	0.8	0.6
723	6.4	2.7	5.9	6.3	5.3	2.1	0.9	1.9	2	1.7
773	20.5	7.2	17.6	12.2	11.5	6.9	2.4	5.6	3.9	3.7
823	40.6	14.4	35.9	19.5	21.6	13.6	4.8	11.5	6.2	6.9

$GHSV_{NH_3}$ = 30,000 ml/(h g_{cat}); the results are averaged data within a TOS of 3 h.

Table 2
H_2 formation [mmol/(min g_{cat})] over supported 4.8 wt.%-Ru catalysts using acetone as solvent

Reaction temperature, K	Ru/CNTs	Ru/MgO	Ru/TiO_2	Ru/Al_2O_3	Ru/AC	Ru–K/CNTs	K–Ru/CNTs
623	2.1	2.0	1.7	1.5	1.3	5.5	8.3
643	3.3	3.1	2.7	2.2	1.9	8.2	12.2
673	5.7	5.4	4.7	3.9	3.8	12.4	19.4
693	–	–	–	–	–	–	25.1
703	9.5	7.7	6.9	5.6	6.3	19.3	28.6
723	14.5	10.3	9.1	7.8	9.6	26.1	32.6
743	–	–	–	–	–	32.2	33.5
753	–	–	–	–	–	33.5	–
773	28.4	23.5	21.7	16.5	21.5	–	–
823	33.4	30.7	29.0	24.7	26.4	–	–

$GHSV_{NH_3}$ = 30,000 ml/(h g_{cat}); the results are averaged data within a TOS of 3 h.

while the Ru/CNTs-a catalyst is superior to the most active Ru/SiO_2 catalyst of Goodman and coworkers.

It has been reported that alkali or alkaline earth ions are efficient promoters for supported Ru or Fe catalysts; they are also effective adjuvants for preventing Ru or Fe from sintering [28,35,42,43,47–49,50]. One can see from Fig. 1 and Table 2 that the modification of CNTs with KOH leads to a better Ru–K/CNTs-a catalyst; compared to the Ru/CNTs-a catalyst, there is a marked increase in NH_3 conversion. When KOH is used to modify a reduced Ru/CNTs-a catalyst, an even better catalyst, viz. K–Ru/CNTs-a is generated. At 673 K, NH_3 conversion over K–Ru/CNTs-a is 59.8%, higher than that over Ru/CNTs-a at 723 K. At 723 K, NH_3 conversion (97.3%) approximates the equilibrium level (99.5%), and H_2 formation rate is 32.6 mmol/(min g_{cat}).

The Ru/CNTs-a, Ru–K/CNTs-a, and K–Ru/CNTs-a catalysts show good durability under reaction conditions (Fig. 2). The activity over Ru/CNTs-a increased slightly but gradually over a reaction period of 26 h. As for the Ru–K/CNTs-a and K–Ru/CNTs-a catalysts, activities remained unchanged over tens of hours. By far, the K–Ru/CNTs-a catalyst is the most active for NH_3 decomposition.

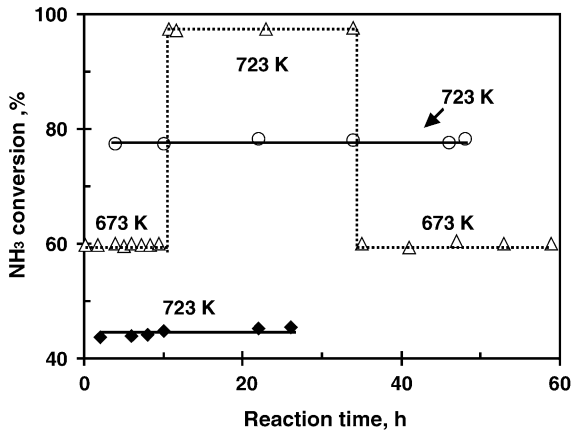

Fig. 2. Stability study of: (◆) Ru/CNTs-a; (○) K–Ru/CNTs-a; (△) Ru–K/CNTs-a catalysts [molar ratio of K:Ru is 1:1, $GHSV_{NH_3}$ = 30,000 ml/(h g_{cat})].

3.2. Characterization

According to the performance of the supported Ru catalysts, one can see that CNTs is the best support material. In order to identify the intrinsic nature of CNTs for such a distinct role, we adopted the following techniques for catalyst characterization.

3.2.1. Temperature-programmed reduction of hydrogen (H_2-TPR)

The results of H_2-TPR studies can provide useful information for catalyst activation by means of H_2-reduction. The technique is often used to examine the strength of interaction between active component and support. Plotted in Fig. 3 are the TPR profiles of the Ru catalysts. The onset temperature for the reduction of the Ru/CNTs precursor using water as solvent is ca. 431 K, and reduction peaks are at 502 K. When acetone is used as solvent, the precursor is more difficult to reduce, and the onset temperature is ca. 448 K, and reduction peaks are at 518 K. Similar phenomena are observed over the precursors of Ru/MgO, Ru/Al_2O_3,

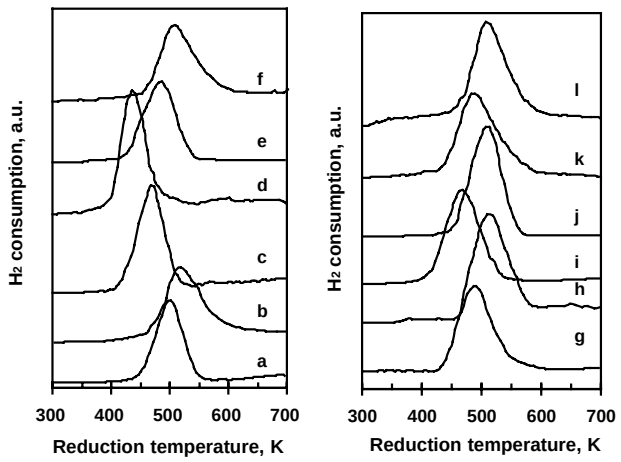

Fig. 3. TPR profiles of supported Ru catalysts: (a) Ru/CNTs-w; (b) Ru/CNTs-a; (c) Ru–K/CNTs-a; (d) K–Ru/CNTs-a; (e) Ru/AC-w; (f) Ru/AC-a; (g) Ru/Al_2O_3-w; (h) Ru/Al_2O_3-a; (i) Ru/MgO-w; (j) Ru/MgO-a; (k) Ru/TiO_2-w; (l) Ru/TiO_2-a.

Ru/AC, and Ru/TiO_2. It seems that compared to the use of water, the use of acetone as solvent would result in stronger interaction between RuO_2 and supports.

It is interesting to notice that with the presence of K^+ ions, the reduction of RuO_2 on CNTs becomes easier. The onset temperatures for the precursors of Ru–K/CNTs-a and K–Ru/CNTs-a are 403 and 381 K, respectively, and maximum reduction occurs at 473 and 436 K. The reduction behavior of precursor is also dependent on support material. For the Ru/support-a catalysts, onset and peak temperatures of precursor reduction can be roughly ranked as CNTs > Al_2O_3 > AC ≅ TiO_2 > MgO; a similar order is observed over the Ru/support-w catalysts. Among the catalysts, the precursor of Ru/CNTs-a is the most difficult to reduce, suggesting that the interaction between RuO_2 and CNTs is the strongest. According to peak area, H_2 consumption was estimated and listed in Table 3. Obviously, the consumption amounts of H_2 over the Ru catalysts are almost identical (900–925 μmol/g_{cat}), independent of support and solvent. We suggest that precursor reducibility is close to 100%.

3.2.2. HRTEM

The HRTEM image (Fig. 4) clearly shows that the adopted carbon tubes have a structure of multiple graphite layers, signifying that the degree of graphitization of the CNTs material is high. The inner diameter of the tubes is within the 3–10 nm range. In comparison, the AC material possesses a lower degree of graphitization. The dark-field image of Ru/CNTs-a shows that despite a small quantity of Ru aggregates, Ru particles are highly dispersed on CNTs, and some Ru particles are with diameter of ca. 2 nm. Since some Ru particles are with size smaller than the inner diameter of CNTs, it is possible to have Ru insertion into the tubes. We observed that the Ru particles are also dispersed well on AC support.

3.2.3. Temperature-programmed desorption of hydrogen (H_2-TPD)

First, H_2-TPD measurements were conducted over pure support materials; the results revealed that H_2 adsorption on the supports is insignificant. Fig. 5 illustrates the desorption behavior of hydrogen from the Ru catalysts. It is evident that H_2 desorption takes place once a sample exposed to H_2 is heated from RT; and the temperature for maximum desorption rate is support dependent. Between the Ru/support-a and Ru/support-w catalysts, desorption temperature and desorption amount are lower over the latter, respectively. The modification of Ru/CNTs-a with KOH results in a shift toward higher temperature in terms of the maximum desorption rate. Despite there is no difference in desorption onset temperature, the temperature for maximum desportion observed in the present study is much lower than that reported over Ru/CeO_2 (588–873 K) by Aika and coworkers [58], and that (573 K) over K–Ru/C by Kowalczyk and coworkers [20].

Based on peak area, the uptakes in H_2 chemisorption can be estimated. Those over Ru/CNTs-a, Ru–K/CNTs-a, and K–Ru/CNTs-a are roughly 100 μmol/g_{cat}, almost double that over Ru/CNTs-w (Table 3). It is apparent that the modification of Ru catalysts with KOH does not result in a remarkable increase of H_2 uptake, a phenomenon similar to that reported over the Ru catalyst supported on AC [50]. The uptakes of H_2 over Ru/AC-a and Ru/CNTs-a are almost the same, indicating that both are suitable support materials for Ru catalysts. Interestingly, for equal support material, the H_2 uptake over Ru/support-w is lower than that over Ru/support-a.

3.2.4. Temperature-programmed desorption of nitrogen (N_2-TPD)

The N_2-TPD patterns of Ru/CNTs-a and K–Ru/CNTs-a are shown in Fig. 6. For Ru/CNTs-a, desorption begins

Table 3
Physicochemical properties of 4.8 wt.% Ru-based catalysts for NH_3 decomposition

Sample[a]	H_2-TPR				H_2-TPD			E_α[c] (kJ/mol)
	Onset reduction temperature (K)	Peak temperature (K)	H_2 consumption (μmol/g)	Reducibility (%)	H_2 uptake (μmol/g)	Peak temperature (K)	Dispersion[b] (%)	
Ru/CNTs-w	441	502	913	98.0	14.2	399	6.1	89.4
Ru/CNTs-a	448	518	907	97.3	49.2	429	21.1	69.4
Ru–K/CNTs-a	414	473	904	97.0	52.9	476	22.7	61.3
K–Ru/CNTs-a	386	436	900	96.6	51.4	513	22.1	55.7
Ru/AC-w	423	484	908	97.4	12.1	378	5.2	85.9
Ru/AC-a	458	514	914	98.1	48.1	420	20.6	74.8
Ru/Al_2O_3-w	433	489	925	99.2	13.9	392	6.0	91.9
Ru/Al_2O_3-a	465	518	917	98.4	23.4	428	10.0	61.2
Ru/MgO-w	414	467	901	96.7	11.7	423	5.0	63.1
Ru/MgO-a	448	508	921	98.8	20.6	460	8.8	61.7
Ru/TiO_2-w	431	491	925	99.2	10.4	397	4.5	75.0
Ru/TiO_2-a	445	511	913	98.0	22.3	439	9.6	60.8

[a] The symbols a and w of the catalyst code represent acetone and water being the solvent for dissolving the $RuCl_3 \cdot xH_2O$ precursor, respectively.
[b] Dispersion was estimated according to H_2 uptake, assuming molar ratio of Ru:H = 1:1.
[c] Apparent activation energy was obtained from the corresponding Arrhenius plots in Figs. 11 and 12.

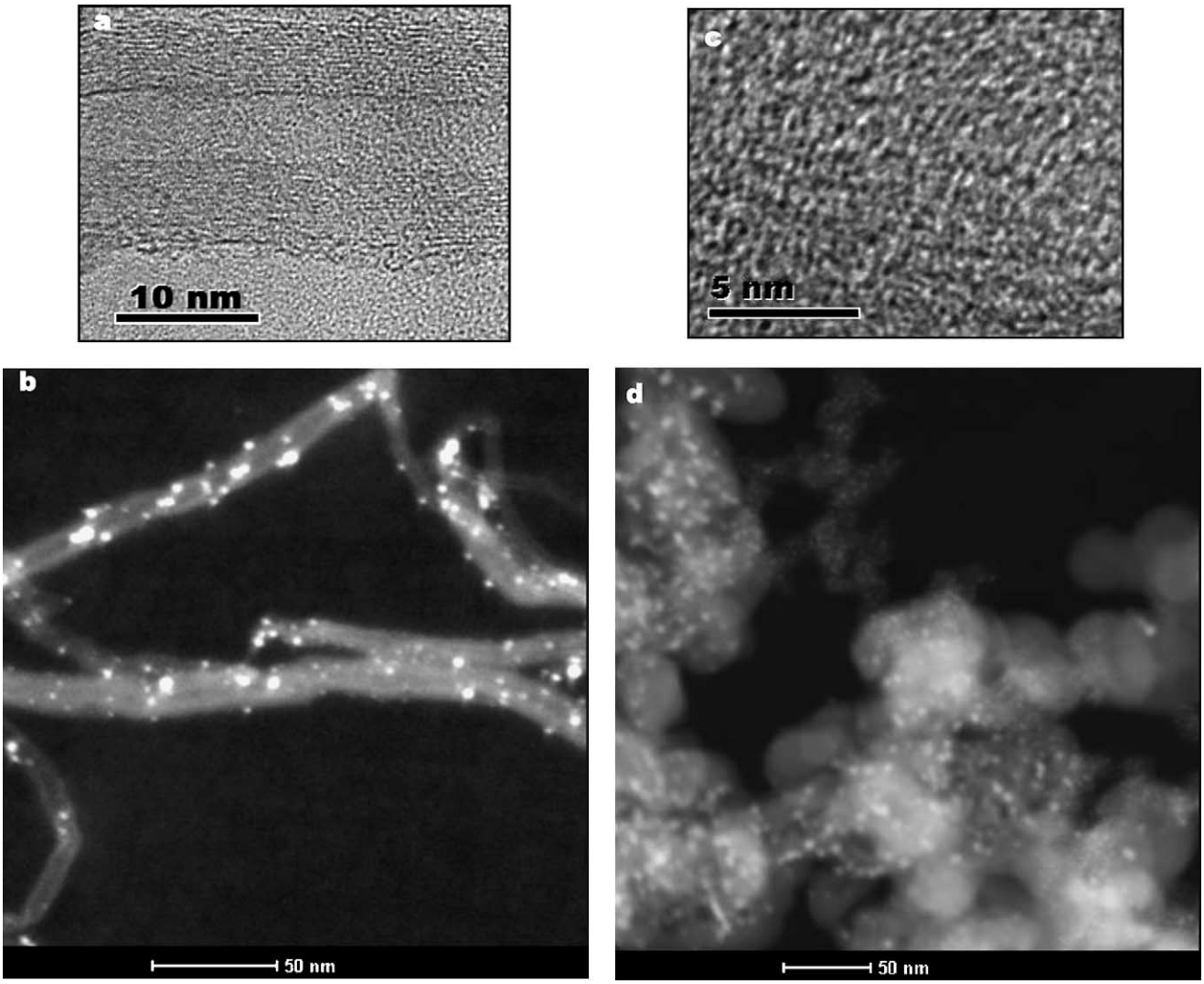

Fig. 4. HRTEM images: (a) CNTs; (b) Ru/CNTs-a (dark-field); (c) AC; (d) Ru/AC-a (dark-field).

at 503 K, and maximum desorption appears at 623 K. With the modification of KOH, maximum desorption over K–Ru/CNTs-a occurs at 583 K, a shift of 40 K to lower temperature in comparison to that over Ru/CNTs-a. Kowalczyk and coworkers [20] reported that N_2 desorption from K–Ru/C started at 473 K and peaked at ca. 623 K. In our study, N_2 desorption amount over Ru/CNTs-a is 29.2 μmol/g, similar to that over K–Ru/C reported by Kowalczyk and coworkers, but ca. 7.7 μmol/g more than that over the K–Ru/CNTs catalyst.

3.2.5. X-ray photoelectron spectrometer (XPS)

The XPS technique was employed to measure the relative molar ratio of chlorine to carbon (Cl/C). Shown in Fig. 7 are the Cl 2p and C 1s spectra of the Ru catalysts. There is no detectable Cl on the purified CNTs, while the Cl/C molar ratios of the freshly reduced Ru/CNTs-a and Ru/CNTs-w catalysts are 5.9×10^{-4} and 1.1×10^{-3}, respectively, confirming that the Cl is from the Ru precursor ($RuCl_3$), and signifying that the use of water as solvent enhances the anchoring of residual chlorine on the supports. The Cl/C ratio of K–Ru/CNTs-a is similar to that of Ru/CNTs-a. However, after 26 h of reaction at 723 K, almost no Cl was detected over the Ru/CNTs-a catalyst, while there was no Cl decrease observed over the used K–Ru/CNTs-a catalyst. The results suggest that the chlorine in Ru/CNTs-a can be removed whereas those in K–Ru/CNTs-a are stable in the course of NH_3 decomposition. In the studies of ammonia synthesis, Cl content was observed to decrease over Ru catalysts supported on carbon black [16], Al_2O_3 [28,29], and MgO [30]. According to Cl 2p peak intensities (Fig. 7), Cl content in Ru–K/CNTs-a ($Cl/C = 5.2 \times 10^{-3}$) is ca. four times that in K–Ru/CNTs-a. Since the Ru/C molar ratio of Ru–K/CNTs-a is 6.1×10^{-3}, the corresponding Cl/Ru molar ratio is 0.85, close to the K/Ru molar ratio (1.0) of the catalyst. The phenomena can be explained by the fact that KOH reacts with $RuCl_3$ to form

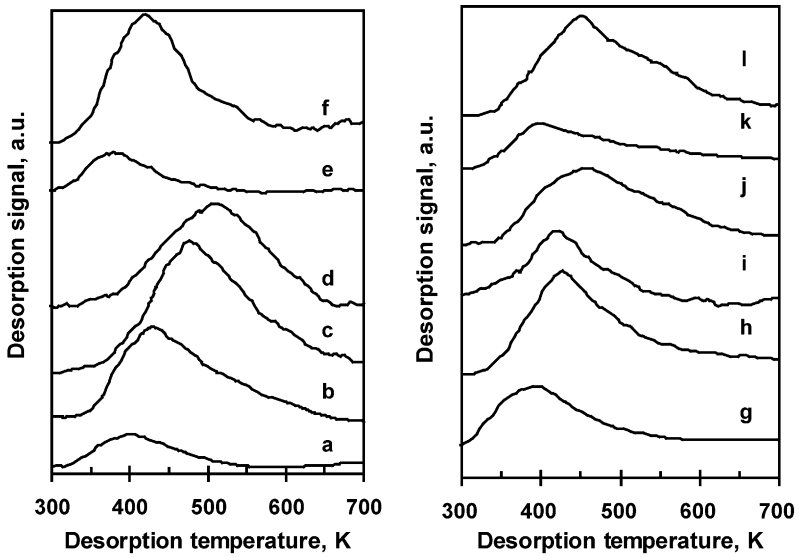

Fig. 5. H_2-TPD profiles of Ru catalysts: (a) Ru/CNTs-w; (b) Ru/CNTs-a; (c) Ru–K/CNTs-a; (d) K–Ru/CNTs-a; (e) Ru/AC-w; (f) Ru/AC-a; (g) Ru/Al_2O_3-w; (h) Ru/Al_2O_3-a; (i) Ru/MgO-w; (j) Ru/MgO-a; (k) Ru/TiO_2-w; (l) Ru/TiO_2-a.

stable KCl. The interaction of residual Cl with $Ba(OH)_2$ has been suggested before by Aika and coworkers [35].

3.2.6. Temperature-programmed hydrogenation (TPH)

The TPH technique was used to study the stability of residual chlorine on CNTs. From Fig. 8, one can see that in a flow of H_2, desorption of HCl (trace amount) began at 640 K over Ru/CNTs-w, and desorption rate increased with a rise in temperature. But, there was nearly no detected HCl from Ru–K/CNTs-a. In order to investigate the thermal stability of KCl entities in the presence of H_2, we conducted the TPH of KCl. We observed that no HCl was produced below 1000 K (note: the melting point and boiling point of KCl are 1043 and 1773 K, respectively). Based on the TPH results, one can conclude that it is impossible to remove residual chlorine in the presence of KOH due to the formation of KCl. In the absence of KOH, it is possible to remove most of the residual chlorine by means of prolonged treatment in H_2 above 640 K.

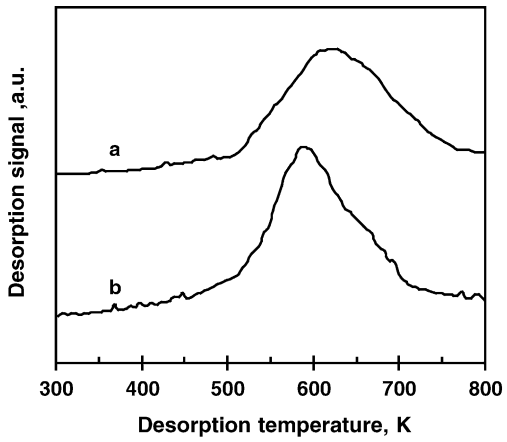

Fig. 6. N_2-TPD profiles of (a) Ru/CNTs-a; (b) K–Ru/CNTs-a catalysts.

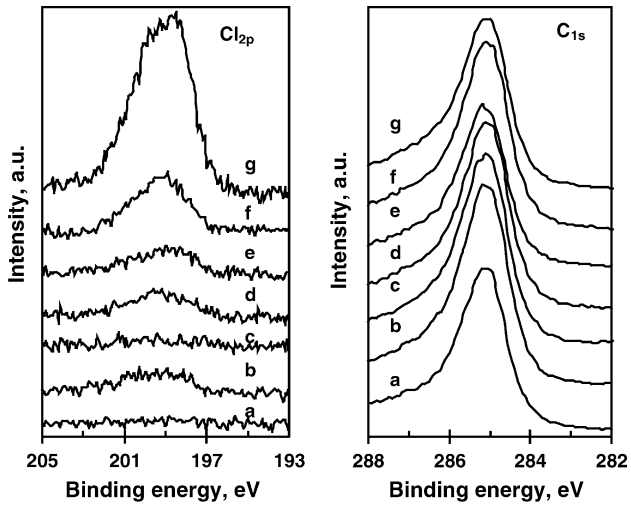

Fig. 7. Cl 2p and C 1s XPS patterns of CNTs-based catalysts: (a) CNTs; (b) freshly reduced Ru/CNTs-a; (c) used Ru/CNTs-a (26 h time-on-steam at 723 K in NH_3 decomposition); (d) fresh K–Ru/CNTs-a; (e) used K–Ru/CNTs-a (26 h time-on-steam at 723 K in NH_3 decomposition); (f) Ru/CNTs-w; (g) Ru–K/CNTs-a.

4. Discussion

4.1. Ru dispersion

According to the chemisorption results, Ru dispersion was estimated assuming an adsorption of one H atom per Ru atom [9,16,19], and the data are listed in Table 3. Obviously, using the same support material, the Ru dispersion

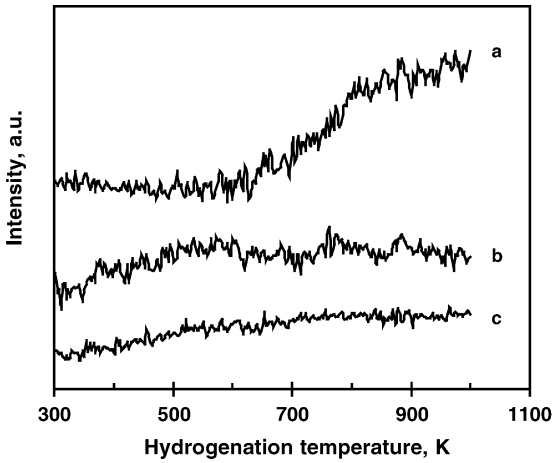

Fig. 8. TPH results of: (a) Ru/CNT-w; (b) Ru–K/CNTs-a; (c) KCl.

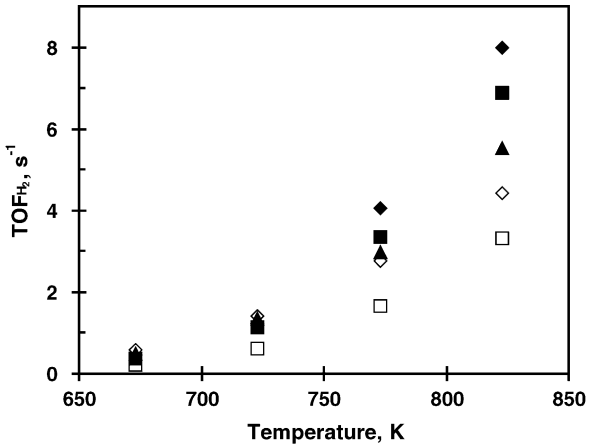

Fig. 9. Comparison of TOFs of H_2 formation over: (◆) Ru/CNTs-w; (◇) Ru/MgO-w; (▲) Ru/TiO_2-w; (□) Ru/AC-w; (■) Ru/Al_2O_3-w. $GHSV_{NH_3}$ = 30,000 ml/(h g_{cat}).

over Ru/support-w is lower than that over Ru/support-a. The data clearly disclose that the use of acetone rather than water as solvent is favorable for Ru dispersion, in agreement with the H_2-TPR results (Fig. 3, Table 3). Both Ru/AC-a and Ru/CNTs-a show a Ru dispersion of ca. 20%, the highest amongst the Ru catalysts. The Ru dispersion of Ru/CNTs-a is higher than those reported by Goodman and coworkers over 10% Ru/SiO_2 and 10% Ru/Al_2O_3 [19]. The Ru dispersions of Ru/AC-a and Ru/CNTs-a are similar to that reported by Bradford et al. over Ru/C [16]. The KOH modification of the CNTs support shows little effect on Ru dispersion.

Generally speaking, a high surface area is favorable for the dispersion of active component. The high dispersion of Ru on AC and CNTs could be partly related to its high surface area. As for CNTs, the material exhibits tube structures of 3–10 nm inner diameter, and Ru location inside the tubes or at the openings of the tubes is possible. The channel and tube sizes can cause restriction to the growth of Ru particles and is beneficial for Ru dispersion. Also, it is known that there are various functional groups (e.g. –COOH, –OH) on carbon materials (e.g. CNTs and AC) [59], and it is possible that these groups are responsible for the anchoring of metal entities. It is also known that these groups show negative effects on electronic structure of Ru. Since the CNTs and AC materials are strongly oleophylic, the use of acetone as solvent for $RuCl_3$ is beneficial for the anchoring of the Ru precursor.

The dispersion of Ru on the metal oxides is in the range of 4.5–10.0% (Table 3), significantly lower than that on the carbon materials; such poor dispersion can be related to the low surface areas of the metal oxides, and the absence of function groups for anchoring Ru particles. Moreover, the Ru dispersion measured by H_2-TPD is close to that determined by H_2- (CO-) chemisorption technique [60].

4.2. Comparison of turnover frequency (TOF)

The turnover frequency (TOF) obtained over a catalyst is often used as a standard parameter for the measurement of catalytic performance. The value is calculated by normalizing the observed reaction rate (mole formed, H_2/s/g_{cat}) to the initial number of exposed Ru surface atoms per gram of catalyst. Figs. 9 and 10 show the effect of support and solvent on the TOF values of the supported Ru catalysts. Clearly, the TOF values over the Ru catalysts are much higher than that reported over the Fe-based catalyst [20]. But unlike NH_3 conversion, the TOF over the Ru/support-a catalysts at 673 K is ranked in the order of Ru/MgO-a > Ru/TiO_2-a > Ru/Al_2O_3-a > Ru/CNTs-a > Ru/AC-a. Similar TOF order is observed over the Ru/support-w catalysts, except that the TOF over Ru/CNTs-w is slightly higher than that over Ru/Al_2O_3-w. It is noted that in our previous study based on XRF technique, after hydrogen reduction at 773 K for 2 h, the concentration of residual Cl on the Ru catalysts is very small, and is independent of the supports (CNTs, MgO, TiO_2, Al_2O_3, ZrO_2, and AC) [60]. Thus, the effect of the residual Cl on the unmodified Ru catalysts in this study

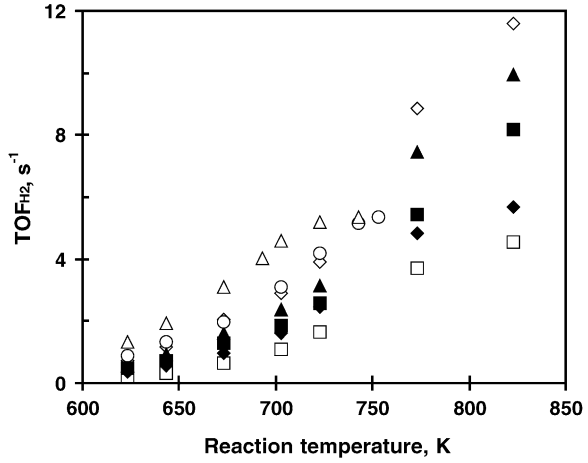

Fig. 10. Comparison of TOFs of H_2 formation over: (◆) Ru/CNTs-a; (◇) Ru/MgO-a; (▲) Ru/TiO_2-a; (□) Ru/AC-a; (■) Ru/Al_2O_3-a; (△) K–Ru/CNTs-a; (○) Ru–K/CNTs-a. $GHSV_{NH_3}$ = 30,000 ml/(h g_{cat}).

is negligible. Despite the NH_3 conversion over Ru/CNTs-a (-w) is higher than that over Ru/MgO-a (-w), the corresponding TOF is in fact lower. Nevertheless, the TOF over Ru–K/CNTs-a is larger than that over Ru/MgO-a under similar reaction conditions. The TOF over Ru/AC-a (-w) is the lowest. In other words, compared to the conventional carbon materials, CNTs is a more suitable support for the Ru catalyst. The specific surface area of AC is much larger than that of CNTs; apparently, there is no direct relationship between TOF and specific surface area. As a matter of fact, the high TOF over Ru/MgO-a (-w) can be related to the basicity of MgO, and the effects of acidity and basicity have been discussed in a separate paper [60]. Compared to the TOF data of (i) the Ir and Ni catalysts using SiO_2 or Al_2O_3 as support [19], (ii) the Fe-based catalysts [20], and (iii) the Cs–Ru/C catalyst [21], the TOF of the present study are much higher. However, it is lower than those of K–Ru/C [22] and Ru/SiO_2 [19]. According to the results of some research works on NH_3 synthesis, higher TOF were observed over catalysts of bigger Ru particles, but accompanied with lower NH_3 yield [28,50,61].

From Figs. 9 and 10, a trend of increase in TOF can be observed over the Ru/support-w and Ru/support-a catalysts, respectively; such a trend can be related to increase in Ru particle size or decrease in Ru dispersion. It seems that similar to NH_3 synthesis [50], the decomposition of NH_3 is structure sensitive. In NH_3 synthesis, Murata and Aika [28] noted a rise in TOF over promoted Ru/Al_2O_3 catalysts when there was a growth in the size of Ru particles. Liang et al. [50] observed that when the size of Ru particles changed from 1.7 to 10.3 nm, TOF increased by a factor of 9 (from 0.004 to 0.036 s^{-1}) over AC-supported Ru. Over Ru/NaX zeolite, upon an increase in Ru particle size by a factor of 3, activity was more than doubled, and TOF increased by a factor of 4 [61]. With regard to Fe catalysts, TOF recorded over large particles is usually higher than that recorded over small particles; it was reported that such effect become really remarkable over the Fe/MgO catalyst in NH_3 synthesis [62].

From the Arrhenius plots (Figs. 11 and 12) based on NH_3 conversion values far away from the equilibrium value, we obtained the related apparent activation energies (E_α). In a previous study of ours, we found that the E_α of unmodified Ru catalyst prepared from acetone solvent is very similar to those obtained over catalysts of smaller size (180–200 mesh) and at higher hourly space velocity of NH_3 [$GHSV_{NH_3}$ = 150,000 ml/(h g_{cat})] [60]. The results suggest that there is no limitation of mass transfer at low NH_3 conversion of the present study, and the obtained E_α data are reliable. One can see from Table 3 that the Ru/CNTs-w catalyst shows an E_α of 89.4 kJ/mol, much higher than that of Ru/CNTs-a (69.4 kJ/mol). The modification of Ru/CNTs with KOH results in a decline in E_α value. Interestingly, on same support basis, the E_α of Ru/support-a is much lower than that of Ru/support-w. It is observed that the E_α of Ru/MgO is the lowest among the Ru catalysts (not counting the KOH-modified ones). The E_α values of the current study are close to those recorded over the Ru catalysts reported by Bradford et al. [16] and Goodman and coworkers [19], but lower than those over K–Ru/C (139 kJ/mol) and K–Fe/C (166 kJ/mol) [21], and those over Cs–Ru/C (134 kJ/mol) and Ba–Ru/C (158 kJ/mol) [22]. It should be pointed out that the difference in apparent activation energy could be due to variation in reaction conditions.

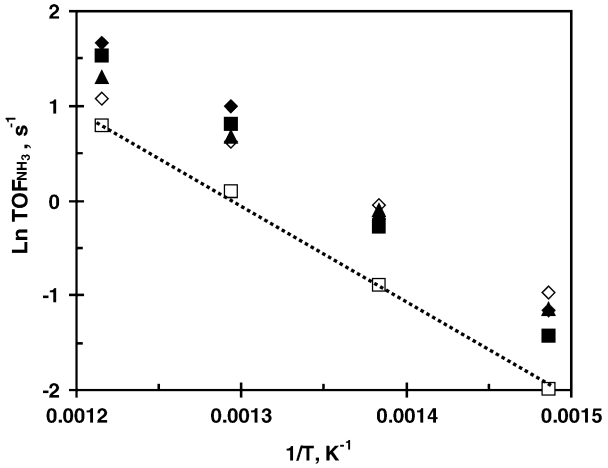

Fig. 11. Arrhenius plots over: (◆) Ru/CNTs-w; (◇) Ru/MgO-w; (▲) Ru/TiO_2-w; (□) Ru/AC-w; (■) Ru/Al_2O_3-w catalysts. $GHSV_{NH_3}$ = 30,000 ml/(h g_{cat}).

4.3. Factors influencing the catalytic performance of Ru/CNTs catalyst

Combining the results of NH_3 conversion, TOF, and catalyst characterization, the factors that affect the catalytic performance of Ru/CNTs are:

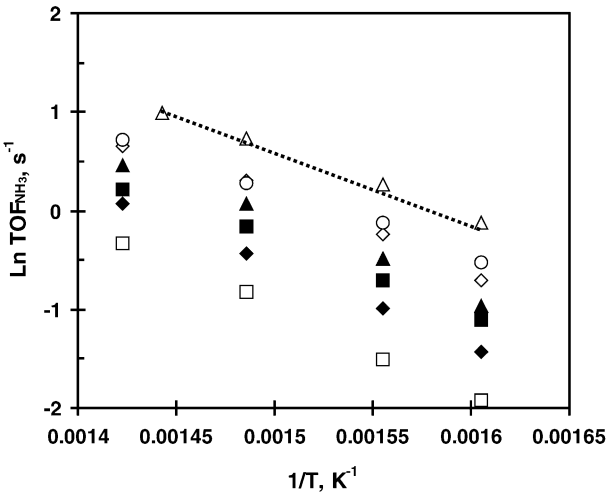

Fig. 12. Arrhenius plots over: (◆) Ru/CNTs-a; (◇) Ru/MgO-a; (▲) Ru/TiO_2-a; (□) Ru/AC-a; (■) Ru/Al_2O_3-a; (△) K–Ru/CNTs-a; (○) Ru–K/CNTs-a catalysts. $GHSV_{NH_3}$ = 30,000 ml/(h g_{cat}).

4.3.1. Ru particle size (dispersion)

The present data clearly show that the NH_3 conversion over Ru/CNTs-a is higher than that over Ru/CNTs-w under similar reaction conditions. Similar phenomena were observed over the other Ru catalysts. The high activity should be ascribed to the high dispersion of Ru when acetone is used as solvent. However, comparing the TOF of the Ru/support-w and Ru/support-a catalysts, we detect low TOF over large Ru particles. As described earlier, the larger Ru particles correspond to higher TOF in NH_3 synthesis [28,50,61]. Such abnormality in the present Ru/CNTs catalyst could be due to residual Cl that imposes an adverse effect on the performance of the catalysts.

4.3.2. Residual Cl

According to the result of XPS measurement, the Cl content on Ru–K/CNTs is higher than that on K–Ru/CNTs, while NH_3 conversion over the former is lower than that over the latter. Moreover, Cl content in Ru/CNTs decreases with reaction time, accompanied with a slow enhancement in catalytic activity. The results indicate that residual chlorine is a strong inhibitor of Ru catalysts, just as reported by Bradford et al. [16], Aika and coworkers [35], Forni et al. [39], etc. Fortunately, most of the residual chlorine in Ru/CNTs is removed as HCl during NH_3 decomposition at 723 K. However, if residual Cl was allowed to react with KOH to form KCl, Cl removal became impossible. We observed that KOH addition does not result in a decrease in Cl content, in disagreement with that reported in the literature [35]. The experimental result of TPH study over KCl provides evidence that KCl is difficult to reduce, even under an atmosphere of H_2. We detected that due to the strong positive effect of the promoters, the negative effect related to chlorine was often overlooked in the studies of promoted catalysts. In the preparation of KOH-modified catalysts, it is wise to treat the materials (CNTs and Ru/CNTs, respectively, in the cases of Ru–K/CNTs-a and K–Ru/CNTs-a) in H_2 for Cl removal before the addition of KOH.

It is obvious that the use of $RuCl_3$ as a precursor inevitably brings about the presence of residual chlorine. Zhong and Aika [34] used Cl-free Ru sources before but organic compounds such as $Ru_3(CO)_{12}$ and $Ru(acac)_3$ are very expensive, and $RuCl_3$ remains as the most common precursor for the preparation of Ru catalysts. In the production of activated carbon, electron impurities (e.g. Cl, S, O, and N) that inhibit nitrogen activation are inevitably present in raw carbon materials [33]. The CNTs material can be free from these impurities if suitable catalyst and carbon source are used in its generation. In addition, carbon loss due to methanation would be an unwelcome problem if the impurities of activated carbon were to be removed by means of hydrogen treatment at 1173 K [33]. Therefore, compared to AC, CNTs is surely a better support for Ru catalysts.

4.3.3. Carbon graphitization

Although the sizes of Ru particles on CNTs and AC are nearly the same, and AC shows a larger specific surface area, both NH_3 conversion and TOF over Ru/AC are lower than those over Ru/CNTs. In the present study, the HRTEM images evidently disclose that the employed multi-wall carbon nanotubes are highly graphitized, while the AC shows a lower degree of graphitization (Fig. 4). This is a possible reason for Ru/CNTs being more active than Ru/AC.

For the use of active carbon as support materials, thermal treatment in an inert atmosphere seems to be necessary for good performance in NH_3 synthesis. Kowalczyk et al. [48,63] reported that high temperature treatment of carbon materials results in higher degree of graphitization, and the use of this material as support yielded a Ru/C catalyst of better NH_3 synthesis activity. The results reported by Rossetti et al. [64] are in concord with such an observation. Based on NH_3 synthesis data obtained over Ru catalysts on carbon supports of various degree of graphitization, Liang et al. [50] reported that a support of higher electronic-conductivity means a better catalytic activity because electron transfer from promoter to Ru is enhanced. It is noted that there are mobile electrons in CNTs. Anyhow, a better understanding of the intrinsic relationship between catalytic activity and degree of support graphitization requires further investigation.

4.3.4. KOH

In previous studies, K, Cs, and Ba were chosen to promote Ru and Fe catalysts for NH_3 synthesis [18,20–22,28–32,39]. Forni et al. [39] monitored the relative promoting effects of Cs, Ba, and K, and found that they could be ranked in the order of Cs > Ba ≥ K. The results of Kowalczyk et al. suggest that the promotion effect should be arranged in the order of Ba > Cs > K, and Ba–Ru/C is more resistant to overheating than K–Ru/C in NH_3 synthesis [21]. They also pointed out that Cs is the best whereas Ba the worst in promoting NH_3 decomposition [47]. We shall conduct investigation on the promotion effects of Cs as well as rare earth compounds in the near future. Furthermore, one should remove residual chlorine before the adding of alkali or alkaline earth metals to the catalyst. Otherwise, the promoting effect of modifiers would be impaired due to residual Cl.

In a study of Ru catalysts for NH_3 synthesis, Liang et al. observed that the Ba and K promoters could cause a change in Ru dispersion [50]. We, however, observed no obvious effect of KOH addition on the dispersion of Ru in the present study. It is worth pointing out that Liang et al. also suggested that the presence of Ba and K would result in the neutralization of surface acidic groups, and a change in surface electron properties of Ru.

The desorption temperature of N_2 over K–Ru/CNTs or Ru–K/CNTs is lower than that over Ru/CNTs, and better activity was observed over the former two catalysts. The results suggest that the desorption of N_2 is the rate-determining

step in NH_3 decomposition. Interestingly, if a comparison were made between the H_2-TPD and N_2-TPD patterns of Ru/CNTs-a and K–Ru/CNTs-a, a higher temperature for H_2 desorption would mean a lower temperature for N_2 desorption and vice visa. The results imply that a strong adsorption of H species on the active sites would facilitate the N_2 desorption process.

Boudart and Djega-Mariadassou [65] proposed that N–H bond cleavage and N_2 desorption are slow irreversible steps in NH_3 decomposition over W and Mo. The results of Löffler and Schmidt [66], Tsai and Weinberg [67], and Bradford et al. [16] over Pt and Ru also support the proposition. Recent results of steady-state isotopic transient analysis provided another piece of convincing evidence in support of the kinetics [68]. The promotion action of alkali metals in NH_3 synthesis is commonly believed to proceed via electron transfer from promoter to Ru metal surface; the result is the lowering of energy barrier for N_2 dissociation, and the destabilization of NH_x and N adspecies [21,28–30]. The kinetics was also used before to explain NH_3 decomposition mechanism and promotion effect of promoters (e.g. K, Cs) [19,20,69].

5. Conclusion

Among CNTs, Al_2O_3, MgO, TiO_2, and AC, CNTs is the best support material for Ru catalysts in NH_3 decomposition. The CNTs material shows a high degree of graphitization, and the CNTs structure restricts the growth of Ru particles. The high activity of the Ru/CNTs can be related to the high dispersion of Ru particles, and to the high graphitization and high purity of the CNTs material. The residual Cl in the Ru catalysts acts as a strong inhibitor. The use of acetone as solvent is beneficial for the formation of small Ru particles. The modification of Ru/CNTs with KOH leads to a remarkable increase in activity and to a decrease in apparent activation energy of decomposition. Our results also support the proposition that desorption of N_2 is the rate-determining step in NH_3 decomposition. The modification with KOH facilitates the desorption of N_2 and hence the decomposition reaction.

Acknowledgements

This work was supported by RGC, Hong Kong Special Administration Region (HKBU 2037/00P), and NSF, PR China (Grant: 20125310) at Tsinghua University. B.Q. Xu thanks the Croucher Foundation for a visitorship to HKBU. We also thank Prof. Wang Shuiju of Xiamen University for the HRTEM analysis.

References

[1] A.S. Chellappa, C.M. Fischer, W.J. Thomson, Appl. Catal. A 227 (2002) 231.
[2] R.O. Idem, N.N. Bakhshi, Ind. Eng. Chem. Res. 33 (1994) 2047.
[3] T.V. Choudhary, D.W. Goodman, Catal. Lett. 59 (1999) 93.
[4] T.V. Choudhary, D.W. Goodman, J. Catal. 192 (2002) 316.
[5] V.R. Choudhary, B.S. Uphade, A.S. Mamman, J. Catal. 172 (1997) 281.
[6] J.N. Armor, Appl. Catal. A 176 (1999) 159.
[7] R. Metkemeijer, P. Achard, Int. J. Hydrogen Energy 19 (1994) 535.
[8] R. Metkemeijer, P. Achard, J. Power Sour. 49 (1994) 271.
[9] W. Arabczyk, J. Zamlynny, Catal. Lett. 60 (1999) 167.
[10] W. Arabczyk, U. Narkiewicz, Appl. Surf. Sci. 196 (2002) 423.
[11] J. Hepola, P. Simell, Appl. Catal. B 14 (1997) 287.
[12] P.A. Simell, J.O. Hepola, A.O. Krause, Fuel 76 (1997) 1117.
[13] G. Papapolymerou, V. Bontozoglou, J. Mol. Catal. A: Chem. 120 (1997) 165.
[14] J.G. Choi, J. Catal. 182 (1999) 104.
[15] K. Hashimoto, N. Toukai, J. Mol. Catal. A: Chem. 161 (2000) 171.
[16] M.C.J. Bradford, P.E. Fanning, M.A. Vannice, J. Catal. 172 (1997) 479.
[17] H. Dietrich, K. Jacobi, G. Ert, Surf. Sci. 352–354 (1996) 138.
[18] W. Arabczyk, J. Zamlynny, Catal. Lett. 60 (1999) 167.
[19] T.V. Choudhary, C. Svadinaragana, D.W. Goodman, Catal. Lett. 72 (2001) 197.
[20] W. Rarog, Z. Kowalczyk, J. Sentek, D. Skladanowski, D. Szmigiel, J. Zielinski, Appl. Catal. A 208 (2001) 213.
[21] W. Raróg, D. Smigiel, Z. Kowalczyk, S. Jodzis, J. Zielinski, J. Catal. 218 (2003) 465.
[22] A. Jedynak, Z. Kowalczyk, D. Smigiel, W. Raróg, J. Zielinski, Appl. Catal. A 237 (2002) 223.
[23] D.A. Goetsch, S.J. Schmit, WO Patent 0 187 770 (2001).
[24] K. Kordesch, V. Hacker, R. Fankhauset, G. Faleschini, WO Patent 0 208 117 (2002).
[25] M.E.E. Abashar, Y.S. Al-Sughair, I.S. Al-Mutaz, Appl. Catal. A 236 (2002) 35.
[26] M.E.E. Abashar, Chem. Eng. Proc. 41 (2002) 403.
[27] C.W. Robert, CRC Handbook of Chemistry and Physics, CRC Press, Florida, D-77, 1983.
[28] S. Murata, K. Aika, J. Catal. 136 (1992) 110.
[29] S. Murata, K. Aika, J. Catal. 136 (1992) 118.
[30] S. Murata, K. Aika, J. Catal. 136 (1992) 126.
[31] K. Aika, J. Kubota, Y. Kadowaki, Y. Niwa, Y. Izumi, Appl. Surf. Sci. 121/122 (1997) 488.
[32] A. Miyazaki, I. Balint, K. Aika, Y. Nakano, J. Catal. 204 (2001) 364.
[33] Z.H. Zhong, K. Aika, J. Catal. 173 (1998) 535.
[34] Z.H. Zhong, K. Aika, Inorg. Chim. Acta 280 (1998) 183.
[35] H.S. Zeng, K. Inazu, K. Aika, Appl. Catal. A 219 (2001) 235.
[36] H.S. Zeng, K. Inazu, K. Aika, J. Catal. 211 (2002) 33.
[37] C.T. Fishel, R.J. Davis, J.M. Garces, J. Catal. 163 (1996) 148.
[38] S. Dahl, P.A. Taylor, E. Törnqvist, I. Chorkendorff, J. Catal. 178 (1998) 679.
[39] L. Forni, D. Molinari, I. Rossetti, N. Pernicone, Appl. Catal. A 185 (1999) 269.
[40] O. Hinrichsen, F. Rosowski, A. Hornung, M. Muhler, G. Ertl, J. Catal. 165 (1997) 33.
[41] H. Bielawa, O. Hinrichsen, A. Birkner, M. Muhler, G. Ertl, Angew. Chem. Int. Ed. Eng. 40 (2001) 1061.
[42] O. Hinrichsen, Catal. Today 53 (1999) 177.
[43] Z. Kowalczyk, Catal. Lett. 37 (1996) 173.
[44] Z. Kowalczyk, S. Jodzis, J. Sentek, Appl. Catal. A 138 (1996) 83.
[45] Z. Kowalczyk, J. Sentek, S. Jodzis, M. Muhler, O. Hinrichsen, J. Catal. 169 (1997) 407.
[46] Z. Kowalczyk, J. Sentek, S. Jodzis, Catal. Lett. 45 (1997) 65.
[47] Z. Kowalczyk, S. Jodzis, W. Raróg, J. Zieliñski, J. Pielaszek, Appl. Catal. A 173 (1998) 153.
[48] Z. Kowalczyk, S. Jodzis, W. Raróg, J. Zieliñski, J. Pielaszek, A. Presz, Appl. Catal. A 184 (1999) 95.

[49] Z. Kowalczyk, M. Krukowski, W. Raróg, D. Smigiel, J. Zieliñski, Appl. Catal. A 248 (2003) 67.
[50] C.H. Liang, Z.B. Wei, Q. Xin, C. Li, Appl. Catal. A 208 (2001) 193.
[51] J.J. McCarroll, S.R. Tennison, N.P. Wilkinson, US Patent 4 600 571 (1986).
[52] L. Duclaux, Carbon 40 (2002) 1751.
[53] J.M. Planeix, N. Coustel, B. Coq, V. Brotons, P.S. Kumbhar, R. Dutartre, P. Geneste, P. Bernier, P.M. Aiayan, J. Am. Chem. Soc. 116 (1994) 7935.
[54] W.Z. Liu, C.H. Liang, J.S. Qiu, W.J. Zhou, H.M. Han, Z.B. Wei, G.Q. Sun, Q. Xin, Carbon 40 (2002) 791.
[55] C.H. Liang, Z.L. Li, J.S. Qiu, C. Li, J. Catal. 211 (2002) 278.
[56] H.B. Chen, J.D. Lin, J. Cai, X.Y. Wang, J. Yi, J. Wang, G. Wei, Y.Z. Lin, D.W. Liao, Appl. Surf. Sci. 180 (2001) 328.
[57] Y. Wang, F. Wei, G.H. Luo, H. Yu, G.S. Gu, Chem. Phys. Lett. 364 (2002) 568.
[58] Y. Izumi, Y. Iwata, K. Aika, J. Phys. Chem. 100 (1996) 9421.
[59] H. Ago, T. Kugler, F. Cacialli, W.R. Salaneck, M.S.P. Shaffer, A.H. Windle, R.H. Friend, J. Phys. Chem. B 103 (1999) 8116.
[60] S.F. Yin, Q.H. Zhang, B.Q. Xu, W.X. Zhu, C.F. Ng, C.T. Au, J. Catal. 224 (2004) 384.
[61] M.D. Cisneros, J.H. Lunsford, J. Catal. 141 (1993) 191.
[62] M. Boudart, A. Delbouille, J.A. Dumesic, S. Khammouma, H. Topsoe, J. Catal. 37 (1975) 486.
[63] W. Raróg, Z. Kowalczyk, J. Sentek, D. Skladanowski, J. Zieliñski, Catal. Lett. 68 (2000) 163.
[64] I. Rossetti, N. Perniconi, R. Forni, Appl. Catal. A 208 (2001) 271.
[65] M. Boudart, G. Djega-Mariadassou, Kinetics of Heterogeneous Catalytic Reactions, Princeton University Press, Princeton, NJ, 1984, p. 98.
[66] D.G. Löffler, L.D. Schmidt, J. Catal. 41 (1976) 40.
[67] W. Tsai, W.H. Weinberg, J. Phys. Chem. 91 (1987) 5307.
[68] B.C. McClaine, R.J. Davis, J. Catal. 211 (2002) 379.
[69] E. Shustorovich, A.T. Bell, Surf. Sci. Lett. 259 (1991) L791.